文章编号: 1001 - 9014(2018)02 - 0168 - 05

DOI:10.11972/j.issn.1001 - 9014.2018.02.007

High power single-higher-mode VCSEL with inverted surface relief

WANG Xia[1], HAO Yong-Qin[1*], YAN Chang-Ling[1], WANG Zuo-Bin[2], WANG Zhi-Wei[1], XIE Jian-Lai[1], MA Xiao-Hui[1*], JIANG Hui-Lin[3]

(1. National Key Laboratory of High-Power Semiconductor Lasers, Changchun University of Science and Technology, Changchun130022, China;
2. International joint Research Centre for Nano Handling and Manufacturing, Changchun University of Science and Technology, Changchun 130022, China;
3. NUERC of Space and Optoelectronics Technology, Changchun University of Science and Technology, Changchun 130022, China)

Abstract: An inverted surface relief vertical-cavity surface-emitting laser (ISR-VCSEL) with annular light emitting window has been presented and investigated. The most prominent structural feature of the device is that the stable single-higher-order transverse mode emission is supported. The laser emits output power up to 9.8 mW at about six times threshold current with an SMSR close to 30 dB, and it can still keep the output power of 4 mW even at as high ambient temperature as 360 K. The measured far field power intensity shows a Gaussian-shaped beam profile with low divergence.

Key words: semiconductor laser, vertical-cavity surface-emitting laser (VCSEL), single-higher-mode, high-temperature, inverted surface relief

PACS: 42.55.Ah, 42.55.Px, 42.60.Pk

高功率单高阶模倒置表面浮雕结构垂直腔面发射激光器

王 霞[1], 郝永芹[1*], 晏长岭[1], 王作斌[2], 王志伟[1], 谢检来[1], 马晓辉[1*], 姜会林[3]

(1. 长春理工大学 高功率半导体激光国家重点实验室,吉林 长春 130022;
2. 长春理工大学 科技部国家纳米操纵与制造国际联合研究中心,吉林 长春 130022;
3. 长春理工大学 空间光电技术研究所,吉林 长春 130022)

摘要:提出并研究了一种带有环形出光孔的倒置表面浮雕结构垂直腔面发射激光器.该器件最突出的结构特点在于,支持稳定的单高阶横向模式激射.在输入电流为六倍阈值电流时,输出功率高达9.8 mW,边模抑制比将近30 dB.在外界为360 K高温时,输出功率仍可达4 mW.且其远场表现出的高斯光束发散角较小.

关 键 词:半导体激光器;垂直腔面发射激光器;单高阶模;高温;倒置表面浮雕

中图分类号:O472+.8 **文献标识码**:A

Introduction

Single mode VCSELs, as the ideal light sources for micro positioning navigation timing, chip-scale atomic clocks (CSACs), the higher data rate communication, optical storage, laser printing, medical diagnosis, airborne Light Detection and Ranging (LIDAR) systems, have become a worldwide hot spot[1-5]. In practical application, low divergence high power single mode VCSELs are usually required, especially single mode operation at high temperatures. While most single mode VCSELs still exhibit low power (several milliwatts), temperature sensitive (multiple modes dominant beyond room temperature or under large injection current), and large beam divergence angle (greater than 10°) due to small emitting areas, all these facts limit the applications in practice. In the system of free-space optical intercon-

Received date: 2017-09-21, **revised date**: 2018-01-12 **收稿日期**:2017-09-21, **修回日期**:2018-01-12

Foundation items: Supported by National Natural Science Foundation of China (11474038/61376045/11474036), the Equipment Pre-research Foundation of China (61424050302162405002), and the "111" Project of China (D17017)

Biography: WANG Xia (1989-), female, Baoding, China, master. Research area involves Semiconductor materials and devices
E-mail: 750239260@qq.com

* **Corresponding author**: E-mail: hyq72081220@aliyun.com, mxh@cust.edu.cn

nects, for example, more complicated beam collimation and coupling is needed, which dramatically enhances the cost of the system. In LIDAR system, it can reduce the spatial resolution. Worse, the temperature sensitivity of the device increases the system cost too.

In order to improve the performance of single mode VCSELs, many innovative ideas have been developed, such as anti-guide VCSEL[6], photonic crystal VCSEL[7], long-cavity VCSEL[8], and SR-VCSEL[9-10], etc. However all these devices provide low power (less than 7.5 mW[6-9, 11-14]) and require rather complicated fabrication steps[15]. Among the various methods, SR-VCSEL is considered to be one of the most efficient methods through partially shallow etch on the surface of a VCSEL. Most SR-VCSELs mainly concentrate on fundamental transverse mode operation[9, 16-19], leading to low output powers, high differential series resistances, tight fabrication tolerances and potentially reduced lifetimes caused by high current densities, due to upper limit of around 5 μm aperture diameter[20]. Furthermore, the divergence angles of output optical beams are usually relatively larger[9]. In contrast, an interesting method is reported to select a single higher-order transverse mode by etching a circle in the center of the emission aperture to form high optical loss region for the fundamental mode[21]. In this work, a single high-order transverse mode ISR-VCSEL with annular light emitting window is demonstrated, and its characteristics are investigated.

1 Device structure and principle

1.1 Device structure

Figure 1 shows the designed schematic illustration of the proposed ISR-VCSEL with annular light emitting window. The bottom n-doped distributed Bragg reflectors (DBRs) consist of 29 pairs of $Al_{0.25}Ga_{0.75}As$/AlAs with quarter-wavelength-thick layers. And then an $Al_{0.6}Ga_{0.4}As$ spacing layer is added, followed by the active region layers. The active region is composed of 7 nm-thick GaAs quantum wells confined by 10 nm-thick $Al_{0.3}Ga_{0.7}As$ barriers to obtain an emission near 850 nm. Like most VCSELs, a 30 nm $Al_{0.98}Ga_{0.02}As$ layer used for the subsequent selective lateral oxidation is placed above the active region. And then the top p-doped DBRs comprising of 21 pairs of $Al_{0.25}Ga_{0.75}As$ and AlAs are deposited. Finally, an $Al_{0.25}Ga_{0.75}As$ antiphase layer with quarter-wave-thick is built, which dramatically increases the top DBRs loss. To attain spatially varied losses at the top DBRs, the antiphase layer is partially dry-chemically etched to form an annular etching region, thus the circular ISR structure serving as a transverse mode discriminator is formed.

1.2 Principle and simulation

(A) Single-mode emission

The transverse optical confinement factor Γ that determines the modal gain is expressed as:

$$\Gamma = \frac{\int_0^a \int_0^{2\pi} \Psi^2(x,y)\,\mathrm{d}x\mathrm{d}y}{\int_0^{\infty} \int_0^{2\pi} \Psi^2(x,y)\,\mathrm{d}x\mathrm{d}y}, \quad (1)$$

where $\Psi^2(x,y)$ is the electric field intensity distribution

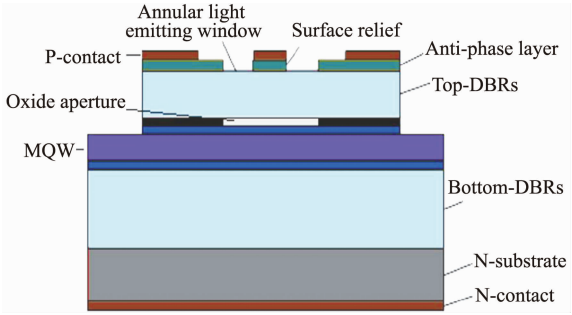

Fig. 1　Schematic cross-section of an ISR-VCSEL with annular light emitting window

图 1　带有环形出光孔的倒置表面浮雕结构垂直腔面发射激光器的示意图

function, and a is the radius of the VCSEL mesa. The higher-order modes are mainly distributed in the annular region, and the fundamental mode is mainly distributed in the central region. Due to the periodic nature of the phase variations, when a layer of 0.5 pairs (quarter-wave-thick) on top of DBRs has been added, which introduce antiphase reflections, the mirror loss reaches a maximum[9, 16]. It is worth noting that the added antiphase layer will be etched to form an annular etching region, differing from the ever reported SR-VCSELs with central etching[16, 22]. So the etched part of the antiphase layer becomes low optical loss region and benefits higher-order modes emitting. In our design, the inside and outside diameters of the annular light emitting area are 5 μm and 15 μm, respectively. And a 15 μm oxide-confined aperture is defined to get good optical and current confinement. Then a single higher-order transverse mode-selection mechanism from an ISR-VCSEL is demonstrated.

(B) Mirror loss

In most VCSELs, the cavity propagation loss is mainly due to the outcoupling through the Bragg mirrors and optical absorption in the semiconductor material. In this paper, we concentrate on the description of the former. Owing to the short gain region in VCSEL, highly reflective mirrors are necessary (reflectivity R > 99%). The transfer matrix is used to calculate the mirror reflectivity of the ISR-VCSEL structure. The reflectivity R at the resonant wavelength of a stack with m pairs is given by[23]:

$$\sqrt{R} = \frac{1 - \frac{n_s}{n_0}\left(\frac{n_1}{n_2}\right)^{2m}}{1 + \frac{n_s}{n_0}\left(\frac{n_1}{n_2}\right)^{2m}}. \quad (2)$$

Here n_0 and n_s refer to the refractive indexes of the incident and substrate media respectively. n_1 and n_2 represent the refractive indexes of the alternate quarter wavelength layers. With an extra half pair added, n_s in Eq. (2) is replaced by n_1^2/n_2, so the reflectivity R can be estimated as:

$$\sqrt{R} = \frac{1 - \frac{n_1^2}{n_s n_0}\left(\frac{n_1}{n_2}\right)^{2m}}{1 + \frac{n_1^2}{n_s n_0}\left(\frac{n_1}{n_2}\right)^{2m}}. \quad (3)$$

Figure 2 shows simulated mirror reflectivity versus the number of pairs. As can be seen, the 29 pairs of bottom-DBRs have the highest reflectivity of 99.99%. The etched part of top-DBRs (21 pairs) also has 99.8% reflectivity enough to meet the lasing condition ($R > 99.5\%$), while the unetched part of top-DBRs (21.5 pairs) has 88% reflectivity only. By partially etching, the annular etched part forms low optical loss region and the unetched area forms high optical loss region, separately. The mode selection from loss mechanism is realized, and lasing can be quenched locally.

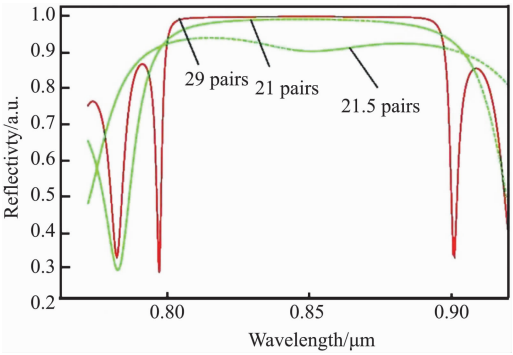

Fig. 2 Reflection spectra of bottom and top DBRs
图2 上下反射镜反射率图谱

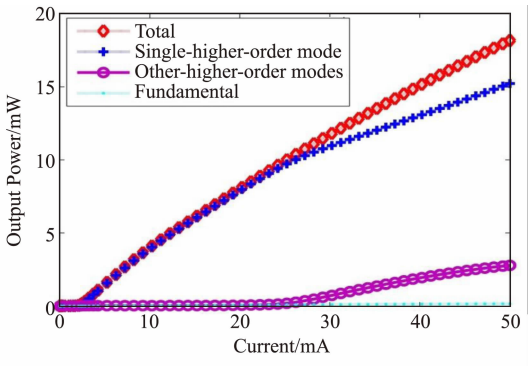

Fig. 3 The simulated *L-I* characteristics of all lasing modes of the device at room temperature
图3 室温下,器件所有模式的 *L-I* 特性曲线

All lasing modes of the device are simulated, as shown in Fig. 3. The device exhibits a single higher-order mode at room temperature under continuous-wave operation with a maximum output power of 15.2 mW@50 mA, accounting for 84% of the total power. The simulated result illustrates that a stable single higher-order mode is attained by the ISR-VCSEL over the entire drive current range. Figure 4 show the near-field (NF) intensity patterns of the device at three different operating currents. A donut-shaped intensity pattern is observed at 20 mA. Fundamental mode and several other higher order modes are absorbed, due to spatially varied losses contrast between etched and un-etched areas in the top Bragg mirror by partially etching, which indicates single higher-order mode is supported. With the current increases, other higher order modes successively appear, while the mentioned single higher-order mode is still dominant, which is consistent with those ever reported near-field distributions[24]. Though the device is similar to ever reported ISR-VCSELs in terms of mode selection mechanism, it supports single higher-order mode lasing rather than the fundamental mode, which brings great changes in its properties, such as output power, temperature sensitivity, and divergence angle.

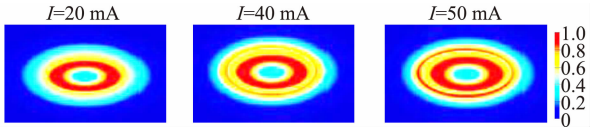

Fig. 4 The near-field (NF) intensity patterns of the device
图4 器件近场模式分布图

2 Experimental results and analysis

Figure 5 depicts the experimental and simulated light-current (*L-I*) characteristics of the ISR-VCSEL at RT under CW operation. The device exhibits a relatively larger threshold current (I_{th}) of 5 mA due to the decreased mirror reflectivity and higher-order mode operation, which is larger than the typical single mode VCSELs, but similar to other SR-VCSELs[9-10, 25]. The maximum output power can reach as high as 9.8 mW at 29 mA. Whereas in Fig. 3, the device exhibits a threshold current (I_{th}) of 3.2 mA, and outputs a maximum power of 18.2 mW at 50 mA. The differences between simulated and measured output power and I_{th} can be attributed to defects in epitaxial growth, optical absorption, and non-uniformity etching. The series resistance is about 100 Ω. For a typical single mode VCSEL, oxide aperture is often limited to 5 μm[20], which leads to a few milliwatts of power and more than 200 Ω resistance[22, 26]. So the higher output power and lower series resistance are attributed to large oxide aperture and the significant large emitting area.

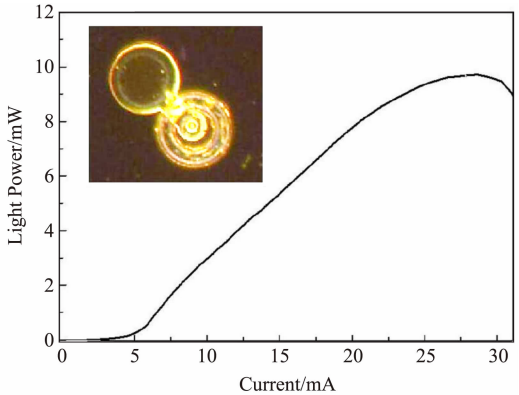

Fig. 5 The output power vs current of the device at room temperature. The inset shows a micrograph of an ISR-VCSEL with annular light emitting window
图5 室温下,输出功率随电流变化曲线;插图为环形出光孔倒置表面浮雕垂直腔面发射激光器显微图

Figure 6 shows CW measured optical spectra of the device at room temperature. The laser exhibits single-mode emission with a side-mode suppression ratio (SMSR) greater than 25 dB throughout the whole current operating range, fulfilling single-mode condition (SMSR ≥ 20 dB)[16, 20-21, 27-31] even at a current of 28 mA, as the result of the strong mode discrimination introduced by the ISR. While most single mode VCSELs show multimode behavior when driven current is above two times threshold[32], the device shows very good single mode performance. With increasing the driving current above threshold, the current leakage and carrier effects, as well as the increased non-radiative recombination, would result in wavelength red-shift.

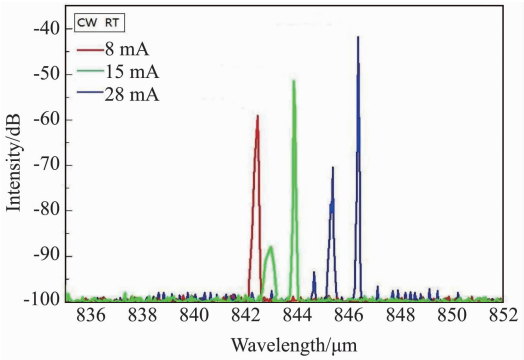

Fig. 6　The measured lasing spectra at different injection current

图 6　激射光谱与注入电流关系曲线

Considering that a certain thermal gradient has an effect on output power and threshold current, measured output characteristics dependent on various temperatures under CW operation are shown in Fig. 7. With the ambient temperature increased, the output power drops, mainly because of the change of average refractive index and the thermal expansion of the semiconductor layers, resulting in the mismatch between the VCSEL cavity mode and maximum optical gain[33]. Nevertheless, there is still power of 4 mW even at a high ambient temperature of 360 K, whereas multimode behavior has been observed at the current of 15 mA, which means that the designed ISR has weak effect in selection mechanism at temperature higher than 360 K. Further improvements to the devices will continue to optimize the cavity design and active regions.

Figure 8 is the measured far-field intensity profiles at different measured currents. The enhanced single-mode operation of the device results in a Gaussian-shaped beam profile with no side-lobes and a high directivity. The divergence angle of single-mode VCSEL can be approximately estimated by Eq. (4). The full-width at half maximum (FWHM) angle is related to the diffraction peaks of order m, operating wavelength λ and outer diameter D[34]:

$$\sin\theta = (2m - 1)\lambda/(2D) \quad . \quad (4)$$

For the case of our demonstrated ISR-VCSE, with outer diameter of 15 μm, the calculated ideal divergence angle is ~1.65°, which is much smaller than the measured results (3.3°). Narrow divergence angle of 7° is

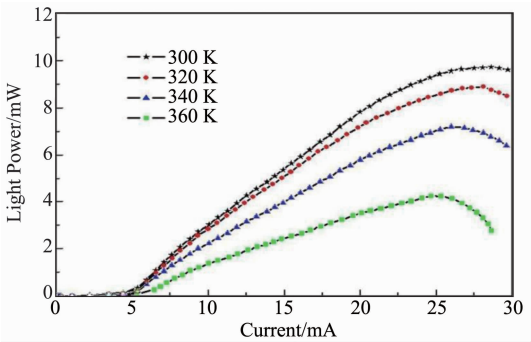

Fig. 7　Optical characteristics of the device at different temperatures

图 7　器件不同温度下的 *L-I* 特性

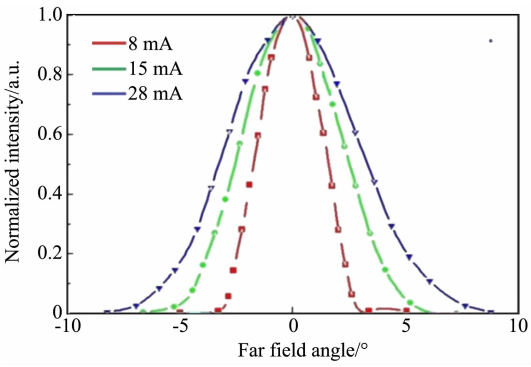

Fig. 8　The measured far-field intensity profiles under different current levels

图 8　不同注入电流下的远场情况

obtained at high injected current of 28 mA, which is much lower than the reported values of previous works on single-mode VCSELs[6,35]. The excellent performance of divergence angle is attributed to larger outer diameter than that of typical single-mode VCSELs.

3　Conclusions

We have demonstrated a single mode ISR-VCSEL. High power of 9.8 mW at about six times threshold current was achieved with an SMSR close to 30 dB. And the laser output power reaches 4 mW even at high temperature of 360 K. The far-field intensity profiles of demonstrated device exhibit single mode performance with a high directivity (a strongly decreased FWHM of 7° even when the current is up to 28 mA). These results show that the device has excellent temperature stability of both output power and optical mode. They, furthermore, imply that a stable single-higher-mode VCSEL can be achieved by ISR VCSEL with annular light emitting window, especially for a wide-temperature-range single mode VCSEL with high power and low divergence.

The ISR VCSEL structure may be used for applications requiring both narrow radiation beam width and high output power. For instance, free-space optical interconnects can benefit from the structure for reasons related to crosstalk and optical efficiency as well as in the system

of LIDAR. The structure provides a guarantee of reliability for the spatial resolution and so on.

References

[1] Huang M C Y, Zhou Y, Changhasnain C J. A surface-emitting laser incorporating a high-index-contrast sub-wavelength grating[J]. *nature*, 2007, **1**(2):119-122.

[2] Haglund Å, Hashemi E, Bengtsson J, *et al*. Progress and challenges in electrically pumped GaN-based VCSELs[C]// *SPIE Photonics Europe*. 2016:98920Y.

[3] Haglund E, Westbergh P, Gustavsson, J S, *et al*. 30 GHz bandwidth 850 nm VCSEL with sub-100 fJ/bit energy dissipation at 25~50 Gbit/s [J]. *Electronics Letters*, 2015, **51**(14):1096-1098.

[4] Iga K. Surface-emitting laser-its birth and generation of new optoelectronics field[J]. *Selected Topics in Quantum Electronics IEEE Journal of*, 2000, **6**(6):1201-1215.

[5] Long C M, Mickovic Z, Dwir B, *et al*. Polarization mode control of long-wavelength VCSELs by intracavity patterning[J]. *Optics Express*, 2016, **24**(9):9715.

[6] Zhou D, Mawst L J. High-power single-mode antiresonant reflecting optical waveguide-type vertical-cavity surface-emitting lasers [J]. *IEEE Journal of Quantum Electronics*, 2002, **38**(12):1599-1606.

[7] Song D S, Kim S H, Park H G, *et al*. Single-fundamental-mode photonic-crystal vertical-cavity surface-emitting lasers[J]. *Applied Physics Letters*, 2002, **80**(21):3901-3903.

[8] Unold H J, Mahmoud S W Z, Jager R, *et al*. Improving single-mode VCSEL performance by introducing a long monolithic cavity[J]. *IEEE Photonics Technology Letters*, 2000, **12**(8):939-941.

[9] Haglund A, Gustavsson J S, Vukusic J, *et al*. Single fundamental-mode output power exceeding 6 mW from VCSELs with a shallow surface relief[J]. *IEEE Photonics Technology Letters*, 2006, **16**(2):368-370.

[10] Jiao J, Wang W, Li L, *et al*. An improved magnetic field detection unit based on length-magnetized Terfenol-D and width-polarized ternary 0.35Pb(In1/2Nb1/2)O3-0.35Pb(Mg1/3Nb2/3)O3-0.30PbTiO3 [J]. *Applied Physics Letters*, 2012, **101**(23):391.

[11] Kroner A, Rinaldi F, Ostermann J M, *et al*. High-performance single fundamental mode AlGaAs VCSELs with mode-selective mirror reflectivities[J]. *Optics Communications*, 2007, **270**(2):332-335.

[12] Furukawa A, Sasaki S, Hoshi M, *et al*. High-power single-mode vertical-cavity surface-emitting lasers with triangular holey structure[J]. *Applied Physics Letters*, 2004, **85**(22): 5161-5163.

[13] Fischer A J, Choquette K D, Chow W W, *et al*. High single-mode power observed from acoupled-resonator vertical-cavity laser diode[J]. *Appl. Phys. Lett.* 2001, **79**(25): 4079-4081.

[14] Shi J W, Chen C C, Wu Y S, *et al*. High-power and high-speed Zn-diffusion single fundamental-modevertical-cavity surface-emitting lasers at 850-nm wavelength[J]. *IEEEPhoton. Technol. Lett.* 2008, **20**(13): 1121-1123.

[15] Kardosh I, Demaria F, Rinaldi F, *et al*. High-power single transverse mode vertical-cavity surface-emitting lasers with monolithically integrated curved dielectric mirrors[J]. *IEEE Photonics Technology Letters*, 2008, **20**(24):2084-2086.

[16] Unold H J, Mahmoud S W Z, Jager R, *et al*. Large-area single-mode VCSELs and the self-aligned surface relief[J]. *IEEE Journal of Selected Topics in Quantum Electronics*, 2001, **2**(2):386-392.

[17] Haglund A, Gustavsson J S, Modh P, *et al*. Dynamic mode stability analysis of surface relief VCSELs under strong RF modulation[J]. *IEEE Photonics Technology Letters*, 2005, **17**(8):1602-1604.

[18] Soderberg E, Gustavsson J S, Modh P, *et al*. Suppression of higher order transverse and oxide modes in 1.3-μm InGaAs VCSELs by an inverted surface relief[J]. *IEEE Photonics Technology Letters*, 2007, **19**(5):327-329.

[19] Xu D W, Yoon S F, Ding Y, *et al*. 1.3-, m In(Ga)As quantum-dot VCSELs fabricated by dielectric-free approach with surface-relief process[J]. *IEEE Photonics Technology Letters*, 2011, **23**(2):91-93.

[20] Jiang C H, Shi J W, Yen J L, *et al*. Single-mode vertical-cavity-surface-emitting[C]// *Quantum Electronics and Laser Science Conference*, 2005. QELS 05. IEEE, 2005, **2**:1026-1028.

[21] Yen J L. Ring shaped vertical-cavity-surface-emitting-laser (VCSEL) with lower divergence angle performance[J]. *Lee-Ming Institute Technol Lett*. 2005, **18**(1):61-66.

[22] Jung C, Jager R, Grabherr M, *et al*. 4.8 mW singlemode oxide confined top-surface emitting vertical-cavity laser diodes [J]. *ELECTRONICS LETTERS- IEE*. 1997, **33**(21):1790-1791.

[23] Sale T E. Cavity and reflector design for vertical cavity surface emitting lasers[J]. *IEE Proceedings-Optoelectronics*. 1995, **142**(1):37-43.

[24] Chang-Hasnain C J, Harbison J P, Hasnain G, *et al*. Dynamic, polarization, and transverse mode characteristics of vertical cavity surface emitting lasers[J]. *IEEE Journal of Quantum Electronics*, 1991, **27**(6):1402-1409.

[25] Kroner A, Kardosh I, Rinaldi F, *et al*. Towards Vcsel-based integrated optical traps for biomedical applications[J]. *Electronics Letters*, 2006, **42**(2):93-94.

[26] Chen C C, Liaw S J, Yang Y J. Stable single-mode operation of an 850-nm VCSEL with a higher order mode absorber formed by shallow Zn diffusion[J]. *IEEE Photonics Technology Letters*, 2001, **13**(4): 266-268.

[27] Bachmann A, Arafin S, Kashanishirazi K. Single-mode electrically pumped GaSb-based VCSELs emitting continuous-wave at 2.4 and 2.6 μm[J]. *New Journal of Physics*, 2009, **11**(12):125014.

[28] Sanchez D, Cerutti L, Tournié E. Single-mode monolithic GaSb vertical-cavity surface-emitting laser.[J]. *Optics Express*, 2012, **20**(14): 15540-6.

[29] Bachmann A, Kashani-Shirazi K, Arafin S, *et al*. GaSb-Based VCSEL with buried tunnel junction for emission around 2.3μm[J]. *IEEE Journal of Selected Topics in Quantum Electronics*, 2009, **15**(3):933-940.

[30] Xiang L, Zhang X, Zhang J W, *et al*. Stable single-mode operation of 894.6 nm VCSEL at high temperatures for Cs atomic sensing[J]. *Chinese Physics B*, 2017, **26**(7):130-133.

[31] Al-Samaneh A, Bou Sanayeh M, Miah M J, *et al*. Polarization-stable vertical-cavity surface-emitting lasers with inverted grating relief for use in microscale atomic clocks[J]. *Applied Physics Letters*, 2012, **101**(17):640-649.

[32] Shi J W, Jiang C H, Chen K M, *et al*. Single-mode vertical-cavity surface-emitting laser with ring-shaped light-emitting aperture[J]. *Applied Physics Letters*, 2005, **87**(3):221.

[33] QU Hong-Wei, GUO Xia, DONG Li-Min, *et al*. Study on the temperature characteristics of vertical cavity surface emitting laser[J]. *Laser & Infrared*(渠红伟, 郭霞, 董立闽,等. 垂直腔面发射激光器温度特性的研究. **激光与红外**), 2005, **35**(2):83-86.

[34] Ebeling K J. *Integrated optoelectronics : waveguide optics, photonics, semiconductors*[M]. Berlin ;New York :Springer-Verlag,c1993.

[35] Young E W, Choquette K D, Chuang S L, *et al*. Single-transverse-mode vertical-cavity lasers under continuous and pulsed operation[J]. *Photonics Technology Letters IEEE*, 2001, **13**(9):927-929.